Vibrational pumping in surface enhanced Raman scattering (SERS)

R. C. Maher,*[a] C. M. Galloway,[b] E. C. Le Ru,[b] L. F. Cohen[a] and P. G. Etchegoin*[b]

Received 7th February 2008
First published as an Advance Article on the web 13th March 2008
DOI: 10.1039/b707870f

In this *tutorial review*, the underlying principles of vibrational pumping in surface enhanced Raman scattering (SERS) are summarized and explained within the framework of their historical development. Some state-of-the-art results in the field are also presented, with the aim of giving an overview on what has been established at this stage, as well as hinting at areas where future developments might take place.

Introduction and motivation

Each Stokes photon in a Raman process leaves an excited vibration behind in the molecule. Vibrational pumping is the significant increase in population of higher excited vibrational states through the strong Stokes scattering characteristic of SERS. The technique is of interest as a fundamental aspect of spectroscopy, but also due to its *potential* as a metrological tool; for it provides—in principle—an estimation of the SERS cross section (*vide infra*).

Like many other topics in SERS, vibrational pumping started with controversy. Kneipp and co-workers first reported evidence of vibrational pumping under SERS conditions in 1996,[1] by studying the power dependence of the anti-Stokes to Stokes (aS/S) ratio (ρ) of rhodamine 6G (RH6G) and crystal violet (CV) using 830 nm laser excitation at room temperature. However, these observations generated much disagreement in the literature, given the relatively large cross sections they suggested and the possibility that other effects might be mis-identified with pumping. Alternative explanations of the data were put forward shortly after the publication of these first results.[2–5] The existence of vibrational pumping in SERS was later confirmed by using an alternative experimental demonstration that overcame all of the initial skepticism by using a different route, as we shall show later.

In this tutorial review, we present an introduction to the basic theory of vibrational pumping under SERS conditions, detailing the different experimental methods to estimate SERS cross sections. We then discuss several experimental results in-and-around the issue of vibrational SERS pumping, and set out some of the advantages and drawbacks of the technique. Finally we conclude the review with a discussion of more advanced and still developing topics such as *single molecule vibrational pumping*, and discuss the future prospects in the field.

Theoretical background

Raman spectroscopy provides a unique spectral fingerprint of vibrations in molecules through inelastic light-scattering. Fig. 1 shows a schematic example of anti-Stokes and Stokes Raman processes. The *efficiency* of the anti-Stokes process is directly dependent on the vibrational population n (Bose factor) of the mode in question. This population of excited states can either be achieved by temperature, or by the laser under SERS vibrational pumping conditions, as we shall illustrate later.

As in any other spectroscopic technique, the efficiency of scattering processes is measured by a cross section, σ [m^2]. Thus the Stokes intensity I_S [W] for an ensemble of N

[a] *The Blackett Laboratory, Imperial College London, Prince Consort Road, London, UK SW7 2BW. E-mail: robert.maher@imperial.ac.uk; Fax: +44-020-75942077; Tel: +44-020-75947563*
[b] *The MacDiarmid Institute for Advanced Materials and Nanotechnology, School of Chemical and Physical Sciences, Victoria University of Wellington, PO Box 600 Wellington, New Zealand. E-mail: Pablo.Etchegoin@vuw.ac.nz; Fax: +64-04-4635237; Tel: +64-04-4635233*

Robert C. Maher is a postdoctoral fellow at the Blackett Laboratory, Imperial College London who is interested in various different applications of Raman spectroscopy such as SERS and other studies on polymers, biomaterials, and fuel cells.

Christopher Galloway is doing a PhD in physics at the School of Chemical and Physical Sciences, Victoria University of Wellington, New Zealand, on the topic of SERS with a particular focus on vibrational pumping.

Eric C. Le Ru is an Advanced Research Scientist at the MacDiarmid Institute for Advanced Materials and Nanotechnology and the School of Chemical and Physical Sciences, Victoria University of Wellington, New Zealand. Eric's interests span several subjects, including plasmonics, SERS, and related spectroscopies (www.victoria.ac.nz/raman).

Lesley F. Cohen is Professor of Experimental Solid State physics at the Blackett Laboratory, Imperial College London, with several different research interests including Raman spectroscopy and SERS (www3.imperial.ac.uk/people/l.cohen).

Pablo G. Etchegoin is a Professor at the MacDiarmid Institute for Advanced Materials and Nanotechnology and the School of Chemical and Physical Sciences, Victoria University of Wellington, New Zealand. His main interests include SERS, Raman spectroscopy of polymers, and isotopically substituted crystals (www.victoria.ac.nz/raman).

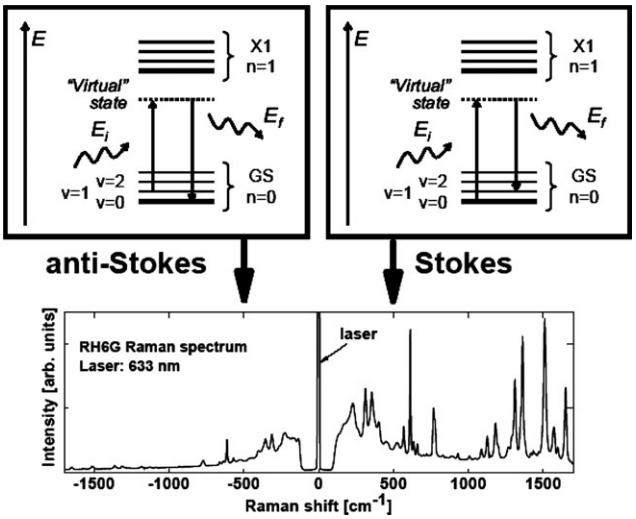

Fig. 1 Schematic (Jablonski) diagrams (top) showing the basic elements of the electronic structure of a molecule. In quantum mechanical terms, a (non-resonant) Stokes process (right) consists of a transition to a *virtual state*, followed by a re-emission, leaving the molecule in the first ($v = 1$) vibrational excited state. This corresponds to *positive* Raman shifts in the spectrum. The anti-Stokes process (negative Raman shifts) on the top-left follows the opposite path, thus producing a photon with a higher energy than the incoming one. The anti-Stokes process depends on the population of the excited level, while the Stokes one is (at low intensities where Raman stimulation is negligible) independent of it. The processes depicted in the top-right (top-left) diagram contribute to the Stokes (anti-Stokes) part of the spectrum at lower (higher) energies with respect to the laser, as depicted in the bottom figure.

molecules illuminated with a laser power density I_L [W m^{-2}], is given by:

$$I_S = N\sigma_S I_L(1 + n) \cong N\sigma_S I_L \quad (1)$$

where σ_S [m^2] is the *Stokes cross section* and n is the population of the vibration (Bose factor). The term n in the factor $(1 + n)$ comes from stimulated scattering, but we shall be working only in cases where $n \ll 1$, thus resulting in $1 + n \approx 1$. The anti-Stokes intensity, on the other hand, is directly proportional to n; *i.e.*:

$$I_{aS} = nN\sigma_{aS} I_L \quad (2)$$

where σ_{aS} [m^2] is the *Anti-Stokes cross section*. In general σ_S will not be exactly the same as σ_{aS}. Even under normal Raman scattering conditions, both cross sections are different (because they depend on wavelength), but under SERS conditions other differences (related to underlying plasmon resonances) might be, in addition, present. We come back to this issue later in the review. If we consider the population of a vibration at temperature T in a SERS experiment, we have (at least) two distinct contributions to n. The first one is the laser itself, which pumps vibrations through Stokes Raman processes with a rate proportional to its power density (I_L) and to the Raman-Stokes cross section (σ_S), *i.e.* a vibration is created for every Stokes scattered photon. The second contribution is the normal thermal excitation of the level. Vibrations remain in a given vibrational level with a finite *vibrational lifetime* τ [s], which encompasses all possible relaxation mechanisms of the population -such as intramolecular vibrational relaxation IVR (anharmonic processes), or external (bath) relaxation mechanisms. Secondary mechanisms, such as relaxation through an anti-Stokes Raman process, or excitation to higher vibrational levels, make a very small contribution. In the case of weak pumping, where the vibrational population remains small, $n \ll 1$, the rate equation for the population reads:

$$\frac{dn}{dt} = \frac{\sigma_S I_L}{\hbar\omega_L} + \frac{e^{-\frac{\hbar\omega_\nu}{k_B T}}}{\tau} - \frac{n}{\tau} \quad (3)$$

where $\hbar\omega_L$ [J] is the energy of an exciting photon, and $\hbar\omega_\nu$ [J] is the energy of the vibration. Very briefly, the first term on the right-hand side is the number of vibrations per unit time being pumped into the level by the action of the laser, while the second and third ones are the contributions of thermal excitation and population relaxation, respectively. In the steady state the condition $dn/dt = 0$ holds. Generally, σ_S is very small, so that the pumping contribution is negligible and the vibrational population is dominated by thermal effects, *i.e.*:

$$n = e^{-\frac{\hbar\omega_\nu}{k_B T}} \quad (4)$$

When I_L or σ_S (through a SERS enhancement) are increased to a level such that pumping makes a significant contribution to the population of the level, n becomes instead (in the steady state):

$$n = \frac{\tau\sigma_S I_L}{\hbar\omega_L} + e^{-\frac{\hbar\omega_\nu}{k_B T}} \quad (5)$$

where the (first) pumping term is clearly distinguished from the thermal contribution (second term).

We can substitute this into the expression for the intensity of the anti-Stokes scattering, given by eqn (2), to obtain:

$$I_{aS} = \left[\frac{\tau\sigma_S I_L}{\hbar\omega_L} + e^{-\frac{\hbar\omega_\nu}{k_B T}}\right] N\sigma_{aS} I_L \quad (6)$$

This shows that the intensity of the anti-Stokes scattering has now two contributions, one proportional to I_L^2 which comes from the population pumped by the laser, and the usual contribution proportional to both I_L and a Boltzmann factor, which comes from the thermal population of the level.

The anti-Stokes to Stokes intensity ratio (ρ)

Taking the ratio, ρ, of the anti-Stokes to the Stokes intensities in the most general case (where contribution from thermal population and/or vibrational pumping might be both present) gives (from eqns (6) and (1)):

$$\rho = \frac{\sigma_{aS}}{\sigma_S}\left[\frac{\tau\sigma_S I_L}{\hbar\omega_L} + e^{-\frac{\hbar\omega_\nu}{k_B T}}\right] \quad (7)$$

The existence of vibrational pumping can hence be demonstrated either by the detection of a quadratic dependence of the anti-Stokes signal on I_L in eqn (6) (plus a linear term if temperature plays a role), or by a linear power dependence of the ratio in eqn (7). We will review these methods in the following Sections.

Under normal Raman scattering conditions, the contribution from the laser to the population is negligible (because σ_S is very small) and ρ reduces to:

$$\rho = \frac{\sigma_{aS}}{\sigma_S} e^{-\frac{\hbar\omega_v}{k_B T}} \sim e^{-\frac{\hbar\omega_v}{k_B T}} \quad (8)$$

where the last equality holds if we ignore the (relatively small) difference between σ_S and σ_{aS}, produced (in non-resonant molecules) by the so-called ω^4-wavelength dependence of all optical cross sections. Eqn (8) is the origin of the use of Raman as a method to measure molecular temperatures with spectroscopy.

Key developments in the field

In this Section we describe within a historical context, the experimental work carried out to investigate vibrational pumping under SERS conditions.

Early observations: measurements as a function of power

The first reports on SERS vibrational pumping focused on the effects of I_L, which can be seen either as a quadratic (added to the normal linear) dependence of the anti-Stokes signal itself in eqn (6), or as a linear dependence of ρ in eqn (7). Since the number of molecules producing a SERS signal N is always very difficult to estimate and/or measure (it cannot be estimated from the average concentration of molecules, due to the presence of very inhomogeneous SERS enhancements), it is more convenient to work with the ratio ρ in eqn (7), which is a *self-normalizing* quantity with respect to N. Ignoring for the moment the difference between σ_S and σ_{aS}, *i.e.* $\sigma_S \sim \sigma_{aS} \sim \sigma$, the coefficient proportional to I_L in eqn (7) is also proportional to both σ and τ. In principle this allows σ to be extracted from the slope of the I_L dependence of ρ, if (and this is a complication we shall revisit later) τ is estimated beforehand. At high temperatures, the large thermal contribution to the vibrational population (last term in eqn (7)) as well as laser heating can produce artifacts, including a linear dependence on I_L. These uncertainties contributed to the initial controversies. The original experiments by Kneipp *et al.* were made using crystal violet (CV) and rhodamine 6G (RH6G) adsorbed onto silver colloids with 830 nm (NIR) laser excitation.[1] Measurements performed under these conditions would be expected to have a substantial contribution from thermal effects. In this initial work, the aS/S ratio of each mode of CV and RH6G was normalised against an aS/S ratio measured under normal Raman scattering for the same experimental conditions. The purpose of this normalisation was to remove any possible errors arising due to the response of the system, and it was defined as:

$$K(\omega_v) = \frac{(I_{aS}^{SERS}/I_S^{SERS})}{(I_{aS}^{RS}/I_S^{RS})} \quad (9)$$

where RS (SERS) means intensities for a specific vibration measured under normal (or SERS) conditions. Normal Raman signals (non-SERS) from CV and RH6G are difficult (but not impossible) to measure due to the small concentrations of dye that can be used and the strong accompanying fluorescence. Because of this, aS/S ratios were obtained from *benzene* under non-SERS conditions and extrapolated to the modes of CV and RH6G; the ratio values for the modes of these molecules were extrapolated from the benzene data. Hence, $K(\omega_v)$ is a measure of the deviation of the vibrational population of the mode under investigation from the Boltzmann factor, which would be expected in normal conditions for non-resonant molecules. From all these combined results the cross section of the vibrational modes under SERS conditions was estimated to be on the order of $\sigma \sim 10^{-16}$ cm^2 by assuming a vibrational lifetime of $\tau \sim 10$ ps. The enhancement factor (F) in SERS is defined as the ratio of the cross section under SERS conditions to that of the normal cross section. The early results on vibrational pumping suggested enhancement factor which were truly remarkable and in the range $F \sim 10^{14}$–10^{15} (for an in-depth discussion of SERS enhancement factors see ref. 11).

Early observations: frequency changes

Further evidence presented in favour of vibrational pumping was based on the assumption that pumping significantly increases the population of the first excited vibrational state. This would allow then for the observation of Stokes scattering from the first ($v = 1$) to the second ($v = 2$) excited states, as well as the standard scattering from the ground state ($v = 0$) to the first excited state ($v = 1$). Given the anharmonic nature of typical vibrational states in molecules, photons scattered from $v = 1$ to $v = 2$ will be at a (slightly) different energy than those scattered from $v = 0$ to $v = 1$. This will result in a slight shift (softening) of the Stokes peak. No shift in energy is expected for the anti-Stokes modes under weak vibrational pumping, as the $v = 2$ level will not be significantly populated and the dominant anti-Stokes process will the $v = 1$ to $v = 0$ transition. Some evidence for frequency shifts of the Stokes peaks were put forward while no detectable changes were observed for the anti-Stokes counterparts, consistent with the above scenario.

Issues with resonances

The reports of optical pumping generated a great deal of interest, tantalising the SERS community with the possibility of estimating the elusive SERS cross sections and enhancement factors. However, Haslett *et al.*[3] were the first to seriously question the existence of vibrational pumping. Extensive measurements were made with a number of both resonant (CV and RH6G) and non-resonant (benzoic acid, phthalazine, pyridine and nitropyridine) molecules under the same experimental conditions as Kneipp *et al.*[1] It was found that only the resonant molecules displayed an anomalous ratio which was independent of power. I_{aS} and I_S were observed to increase linearly with power until photodecomposition occurred for all modes of all the investigated analytes. These observations suggested that the effect was purely a resonance effect. Moskovits *et al.* also cast serious doubts on the claimed order of magnitude of the enhancements[6] arguing that there is no known physical mechanism capable of achieving the $F \sim 10^{14}$–10^{15} SERS enhancements claimed in many reports. Furthermore, it was argued that, were they real, it would imply electric field intensities that would completely destroy the chemical identity of the probes.

Alternative scenarios: the heating problem

Brolo *et al*. proposed direct laser heating of the molecule as an alternative explanation to the power dependent behaviour observed.[4] They showed explicitly how the presence of resonance + heating effects could produce an anomalous ratio by expanding the expression for $K(\omega_\nu)$ (eqn (9)) to include simultaneously the effects of resonances and temperature.[4] In order to better understand the effect of heating on ρ, we give a simplified version here: we can write $T = T_0 + \Delta T$, and expand eqn (8) (when pumping is negligible or non-existent) considering a small temperature increase, $\Delta T \ll T_0$ to obtain:

$$\rho \sim \mathrm{e}^{-\frac{\hbar\omega_v}{k_\mathrm{B}T_0}}\left(1+\frac{\hbar\omega_v\Delta T}{k_\mathrm{B}T_0^2}\right) \qquad (10)$$

Because heat diffusion and transfer models are linear, the temperature increase ΔT is proportional to laser power density; *i.e*. $\Delta T = aI_\mathrm{L}$, where a is a coefficient. Hence, for a small temperature increase we obtain:

$$\rho \sim \mathrm{e}^{-\frac{\hbar\omega_v}{k_\mathrm{B}T_0}}\left(1+\frac{\hbar\omega_v\Delta T}{k_\mathrm{B}T_0^2}I_\mathrm{L}\right) \qquad (11)$$

The linear dependence of ρ with incident power density can, therefore, equally be the result of *conventional heating effects* or of *pumping*. This shows that heating effects can be important, and that a linear power dependence of ρ is not in itself a proof of vibrational pumping. Moreover, it is worth noting that the coefficient before I_L in eqn (11) depends on the mode energy, and will be more important for high energy modes, thus potentially explaining also the mode-dependent behaviour of the ratio observed experimentally in the early attempts.

In fact, to make eqn (7) completely general, any possible laser heating of the analyte above the bath temperature T must be included. This is achieved by replacing T by $T_0 + \Delta T$ where T_0 is the bath temperature (measured by a thermometer in the sample holder, for example) and ΔT is the increase in analyte temperature due to the laser. It is clear from eqn (11) that heating must be eliminated from the experiment in order to put the experimental observation on firm grounds. It can also be mentioned in passing that frequency shifts can also be ascribed to the combination of laser heating and anharmonic interactions among modes. Even if transitions from $v = 1$ to $v = 2$ due to pumping (as described in the previous subsection) were present, heating needs to be discounted as the possible reason for the softening of modes.

Measurements as a function of temperature

The study of the temperature dependence of ρ overcomes many of the difficulties which we have discussed above. The main reason why vibrational pumping is so difficult to identify at higher temperatures is because it involves the study of *small departures in mode population* from the *large thermal population* already existing in the levels. However, given the exponential dependence of the thermal contribution to the vibrational population, it is possible to reach a regime where thermal effects are completely negligible compared to vibrational pumping. It all comes down to the interplay between the first and second right-hand terms in eqn (7). The use of a fixed power throughout the measurement is required and this can be made as small as the signals allow. This reduces the contribution from laser heating to a negligible level and ensures that the sample is as stable as possible (photobleaching).

Fig. 2 presents a schematic view of the possible results of a measurement of ρ as a function of temperature. The solid lines show the variation of the ratio with T when pumping is absent. In this case ρ decreases exponentially with T, as expected from the Boltzmann factor $\exp(-\hbar\omega_\nu/k_\mathrm{B}T)$. The dashed lines show the case when pumping is present, *i.e*. both terms in eqn (7). At high T's the ratio is approximately the same as if pumping were absent, and hence this is the *thermally-dominated regime*. As T is decreased the thermal contribution decreases exponentially, whilst the pumping contribution remains constant. Eventually the pumping and thermal contributions will become comparable, and there is a cross-over to a *pumping-dominated regime* where the ratio reaches a plateau. The temperature at which this occurs is indicated by arrows in Fig. 2, and is referred to as the cross-over temperature T_cr, where the pumping and thermal terms in eqn (7) are comparable. T_cr is given by:

$$k_\mathrm{B}T_\mathrm{cr} = \hbar\omega_v\left[\ln\left(\frac{\hbar\omega_\mathrm{L}}{\tau\sigma_\mathrm{S}I_\mathrm{L}}\right)\right]^{-1} \qquad (12)$$

The cross-over occurs at higher temperatures not only for higher laser intensities, I_L and higher σ_S's (for which the contribution of pumping is stronger) but also for higher energy peaks (with a larger $\hbar\omega_\nu$), for which the contribution to the thermal population of the level becomes much weaker at higher temperatures (compared to modes with smaller $\hbar\omega_\nu$'s). In the pumping-dominated regime, ρ is constant and given by:

$$\rho = \frac{\tau\sigma_\mathrm{aS}I_\mathrm{L}}{\hbar\omega_\mathrm{L}} = \frac{A\tau\sigma_\mathrm{S}I_\mathrm{L}}{\hbar\omega_\mathrm{L}} \qquad (13)$$

where A is the *asymmetry factor* ($A = \sigma_\mathrm{aS}/\sigma_\mathrm{S}$) measuring the difference between σ_S and σ_aS produced either by their intrinsic frequency dependences (ω^4-factor) or by the presence of

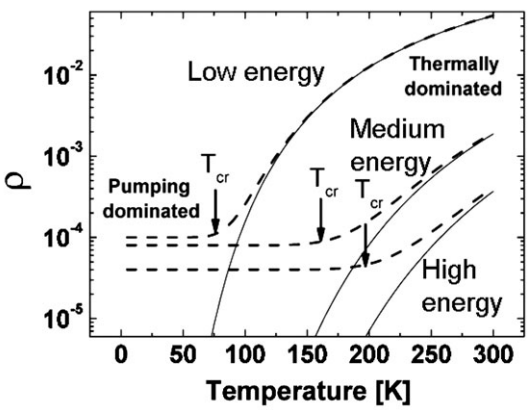

Fig. 2 Schematic diagram showing the temperature dependence of ρ for low, medium and high energy Raman modes (assuming similar but not identical cross sections and lifetimes for them) at fixed I_L. The solid lines represent the ratio when there is no pumping (Boltzmann factor). The dashed lines show the result of including pumping as given by eqn (7). The cross-over point, T_cr, between the pumping and thermally dominated regimes is indicated by the arrows.

underlying plasmon resonances making the enhancement at the Stokes frequency different from that at the anti-Stokes one. There is another potential *intrinsic* contribution to the asymmetry factor which goes beyond the ω^4-factor and is related to *resonance* or *pre-resonance* conditions in the molecule itself. It is well known, for example, that the Raman spectrum of RH6G at 633 nm under non-SERS conditions has differences between σ_S and σ_{aS} for most modes that cannot be accounted for *solely* by the ω^4-factor; they come from *pre-resonance* effects and the fact that the anti-Stokes side is closer to a resonance condition than the Stokes one. As $I_L/\hbar\omega_L$ [photons m^{-2} s^{-1}] can be estimated to a very high degree of accuracy for given experimental conditions, we can deduce the product $\tau\sigma_{aS}$ (or $A\tau\sigma_S$) from the plateau in the aS/S-ratio (ρ) below T_{cr}.

Hence, temperature dependent measurements (or low temperature measurements) of ρ makes the investigation of optical pumping easier, more reliable, and greatly simplifies the interpretation compared to room-temperature power dependent studies. The appearance of a plateau for $T < T_{cr}$ in an experimental measurement represents a conclusive demonstration of vibrational pumping. This would not mean that heating is absent, but simply that its effect on ρ, relative to that of optical pumping, is negligible. Whilst any heating effects may affect the value of T_{cr}, a plateau will only be observed if vibrational pumping is present, and it will happen at different temperatures for different modes depending on the mode energy $\hbar\omega_\nu$ and its corresponding cross section σ_S and lifetime τ; with the predominant factor being normally the mode energy.

Quantifying resonance effects

As we have seen in the previous sections, resonances can play a significant role in SERS experiments. It is not enough to merely consider the analyte itself as the resonance properties of the metallic substrate will also play a role in the measurement. For silver colloids, for example, the number and variety of resonances that can appear due to clustering and *collective* resonance effects is enormous and they span the whole visible range up to the near-IR (NIR).

It is relatively easy to understand how resonances can result in anomalous anti-Stokes/Stokes intensities by considering their effect on the SERS cross sections. Fig. 3(a) shows a simple example of how the enhancement can vary as a function of wavelength in the presence of a hypothetical resonance, and exemplifies their possible effects on measurements made with different lasers. For a plasmon resonance peaking in the yellow region of the spectrum (a fairly common experimental case) the 514 nm laser would see that the anti-Stokes is enhanced to a lesser degree than the Stokes side, thus resulting in an anomalous ratio (smaller than expected). The opposite occurs for measurements using, say, a 633 nm laser in the red, thus resulting in a *larger than expected ratio*. The wavelength dependent normalized ratio over the same range as the enhancement profile is also shown in Fig. 3(b).

Such resonance contributions must then be included in the theoretical treatment of vibrational pumping if an accurate description is sought. Resonance effects are absorbed (in the present formalism) in the *asymmetry factor A* defined previously (*vide supra*), allowing any difference in the anti-Stokes, σ_{aS}, and Stokes σ_S cross sections (beyond and including the normal ω^4-correction plus resonance or pre-resonance effects on the intrinsic cross section).

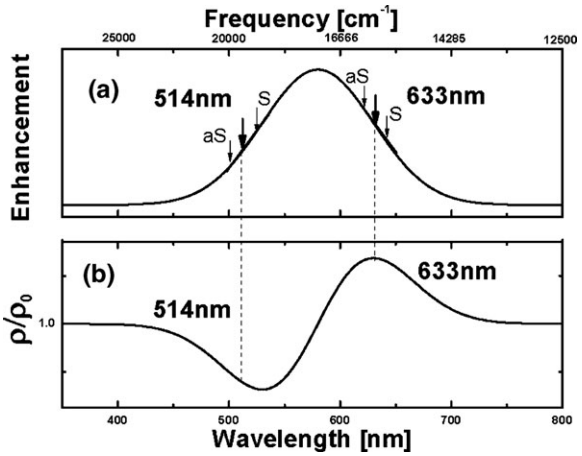

Fig. 3 Schematic diagram showing (a) enhancement profile by a plasmon resonance in a SERS substrate, and (b) the normalized aS/S ratio in the presence of the resonance. Values which are *higher* than normal can be obtained *only* by resonance effects and the asymmetry of the cross sections, without invoking any effect from pumping.

Including explicitly the asymmetry factor A and the possibility of small laser heating by ΔT from a nominal temperature T_0, the expression of the aS/S-ratio including vibrational pumping and thermal population reads:

$$\rho = A\left[\frac{\tau\sigma_S I_L}{\hbar\omega_L} + e^{-\frac{\hbar\omega_\nu}{k_B(T_0+\Delta T)}}\right] \qquad (14)$$

In the next section we will review our own experimental work on the investigation of vibrational pumping as a function of temperature under different experimental conditions.

Temperature dependences

Fig. 4 shows anti-Stokes and Stokes spectra for the 610 and 1650 cm^{-1} Raman modes of RH6G on silver colloids (10 mM KCl dried on Si-wafers with 1 μM dye concentration) for 676 nm laser excitation (Kr^+-ion laser, $I_L = 1.6 \times 10^8$ W m^{-2}, spot size ~10 μm in diameter) measured at 300 and 10 K. At 300 K the peaks show the normal aS/S ratio modified by the asymmetry factor A only. The Stokes side remains relatively constant throughout the measurement, as can be seen in the data. This implies that photobleaching effects are negligible under these experimental conditions. At T = 150 K (not shown) an anomalous relative intensity between the two peaks on the anti-Stokes side can already be seen; while the anti-Stokes signal of the 610 cm^{-1} mode still decreases the 1650 cm^{-1} mode remains visible and constant on the anti-Stokes side (at a temperature where the population of this level suggests it would not be observable). This is because the pumping term already dominates at this temperature for this mode, whilst the 610 cm^{-1} mode is still affected by thermal contributions (and still shows a dependence on T). At T = 10 K, the anti-Stokes signals of both peaks are almost comparable in size, despite the Boltzmann factors for these

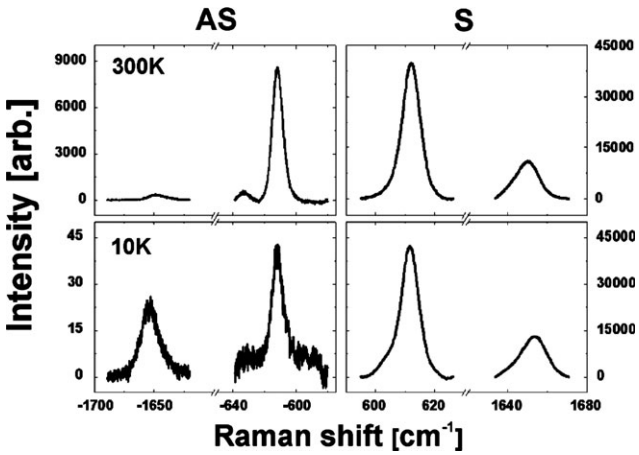

Fig. 4 Anti-Stokes (left) and Stokes (right) spectra for two widely separated modes of RH6G (610 cm^{-1} and 1650 cm^{-1}) under 676 nm laser excitation. The top (bottom) plots show data at T = 300 K (10 K). The anti-Stokes signals at T = 10 K are only visible because of vibrational pumping and the signals have already reached the plateau region in ρ.

two peaks being $\sim 10^{-38}$ (610 cm^{-1}) and $\sim 10^{-100}$!! (1650 cm^{-1}) at 10 K, respectively. It is only because of vibrational pumping that they are still visible.

Fig. 5 shows the experimental values of ρ (plotted as $\ln(\rho)$ *vs.* T) obtained for *four* different modes of RH6G as a function of temperature, for 676 nm laser excitation (same conditions of Fig. 4). The temperature at which a crossover between the *pumping* and *thermal dominated* regimes occurs is shown by the vertical arrows. The cross-over clearly occurs at higher T's for vibrational modes with larger energies. The observation of a clear mode-dependent crossover between the two regimes is a sound demonstration of the existence of SERS vibrational pumping.

The first step from here to extract estimates of the cross section is to fit the experimental data to eqn (14). Initially, fits are done for $\Delta T = 0$, unless the data explicitly forces the existence of laser heating to be considered. This is not generally an issue at the very low power densities in which these experiments are carried out. It is convenient to transform

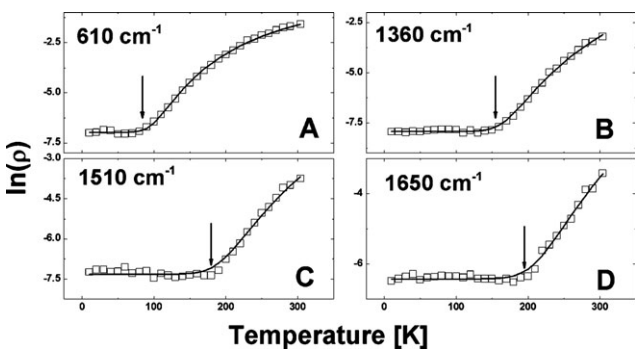

Fig. 5 Anti-Stokes/Stokes ratios ($\ln \rho$) as a function of T for four modes of RH6G (under 676 nm laser excitation). Note that the crossover happens at different temperatures for different modes (vertical arrows), being at higher T's for larger vibrational energies. The solid lines are fits using eqn (15).

eqn (14) (with $\Delta T = 0$) to:

$$\ln(\rho) = \ln(a) + \ln\left[b + e^{-\frac{\hbar\omega_v}{k_B T}}\right] \qquad (15)$$

where $a = \ln(A)$, and $b = \tau\sigma_S I_L/\hbar\omega_L$ are two *dimensionless* parameters obtained from the fit. The τ's of the vibrational modes are necessary to obtain the Stokes cross sections from the dimensionless parameter b. The issues associated with extracting the cross section from these measurements are extensive, and are the subject of the following section.

Cross section estimations

In practice, there are several complications with the estimation of cross sections using vibrational pumping, including the *statistics of the distribution of enhancements* and the *estimation of the vibrational lifetime* τ. We will show why these issues are so important in order to understand the real meaning of the cross sections extracted from this method and their limitations.

Lifetime estimations

In order to extract cross sections from any experiment using SERS vibrational pumping, τ needs to be known. However, there are many drawbacks to simplistic estimations of τ, such as inconsistencies between the value of the cross section extracted from different modes and the relative intensities of these modes in the Stokes spectrum (*i.e.* one would expect a higher relative Stokes amplitude for a mode that shows a high cross section value). Ideally direct measurement of the vibrational lifetime using time resolved spectroscopy[7] would resolve this problem. However, this has never been attempted under SERS conditions, to the very best of our knowledge.

One possible alternative is the estimation of the lifetime from the full-width-at-half-maximum (FWHM), Γ, of the peaks using $\tau \sim \hbar/\Gamma$. However, Raman modes are seldom pure Lorentzians and have several contributions to their natural linewidths[7] including (i) overlapping Raman modes, (ii) inhomogeneous broadening, (iii) phase coherence relaxation, and (iv) population relaxation. The last two are also known as the off-diagonal (dephasing) and diagonal (population) relaxation times in density matrix formalism,[7] respectively, and are part of the homogeneous broadening of the peak.[8] These relaxation times are, in principle, different for each mode and cannot be separated from the observed linewidth in a plain SERS spectrum. Thus, an estimation of τ directly from Γ will be an underestimation, and will result in cross section values that are not precisely consistent with the relative intensities of the Raman modes.

By way of compromise, we can use the Raman mode for which population relaxation contributes most strongly to the width as a *reference mode*, in order to extract the values of the other cross sections. In order to find which mode has the strongest contribution from population relaxation we use an iterative process that starts with the highest energy mode. Once the reference mode is chosen we can calculate its lifetime *via* $\tau \sim \hbar/\Gamma$, which is then used to determine the cross sections of the ith peak (σ_S^i) through their relative

Table 1 Values of b, τ, Rel. I_S, Rel. σ_S, σ_S and σ_{aS} of the Raman modes of RH6G adsorbed on Ag colloids using the 676 nm excitation with τ estimated using the CLM. See text for further details

Mode/cm^{-1}	$10^5 b$	τ/ps	Rel. I_S	Rel. σ_S	$10^{15}\sigma_S$/cm^2	$10^{15}\sigma_{aS}$/cm^2
610	25.6	10.4	0.9	0.9	0.5	1.7
780	6.9	2.3	1.1	1.1	0.6	2.7
1360	1.3	0.5	1.0	1.0	0.5	14.3
1510	2.1	0.4	1.7	1.7	0.9	28.3
1650	2.1	1.3	0.6	0.6	0.3	23.5

Stokes intensities from:

$$\sigma_S^i = \frac{I_S^i}{I_S^{\text{Ref.}}}\sigma_S^{\text{Ref.}} \tag{16}$$

where the cross section and lifetime of the reference peak are $\sigma_S^{\text{Ref.}}$, and $\tau^{\text{Ref.}}$, respectively, and I_S^i and $I_S^{\text{Ref.}}$ are the integrated Stokes intensities of the ith peak and reference peak, respectively. The lifetimes, τ_i, can only be larger or equal to that estimated from $\hbar/\Gamma_i$. Thus, to ensure the consistency of the obtained σ_S^i, the τ_i's for each mode are checked to ensure that they are larger than the value of τ obtained from their widths Γ^i. If this is not the case, the choice of the reference mode was not the most appropriate. The strategy is then to go to the next lowest mode and repeat the estimation of lifetimes until this last condition is fulfilled. We refer to this method as the *corrected lifetime method* (CLM), but it has to be clear that it is an approximation that might not be always valid and it has to be judged on a case-by-case basis. It is, in particular, based on the assumption that at least one of the modes has its broadening dominated by population relaxation (rather than dephasing). If this is not the case, all the cross-sections will be overestimated.

Table 1 shows the results of fitting the experimental data for RH6G on dried silver colloids (Lee and Meisel[9]) taken with the 676 nm line. A column with relative intensities and cross sections among modes is also provided for completeness. The anti-Stokes cross sections are obtained through the Stokes ones *via* the fitted value of the asymmetry factor A from eqn (15). The values estimated with vibrational pumping are always at the *upper limit* of what is expected in these substrates; *they are typical values of single-molecule SERS cross sections*. This is due not only to the uncertainty in the estimation of the τ's, but also due to additional effects with the averaging of the cross section over the enhancement distribution, as discussed in the next section. The overestimation can also come from *other pumping channels* not considered in the present formalism, such as *fluorescence pumping* considered later in the framework of single molecule pumping.

Enhancement distribution averaging

The cross sections extracted from the experimental data of vibrational pumping are (typically) at the higher end of the accepted values for SERS conditions and only valid within the approximations made. The first obvious question we need to address now is: do we obtain an estimate of the average cross section with this method?

It is generally accepted that SERS signals are dominated by the presence of "hot-spots" or places with high local enhancements. The formulae presented above made the implicit assumption that the cross section is the same for all N molecules in the sample. We shall show in what follows that what we actually obtain from the experiment is an estimate which is heavily biased towards the sites with the highest enhancements; *i.e. the method provides (at best) an estimate of the cross-sections of hot-spots*.

We consider a number of molecules (i from 1 to N) in the sample. Each molecule can have a different anti-Stokes, (σ_{aS}^i) and Stokes (σ_S^i) SERS cross sections (and a corresponding asymmetry factor $A^i = \sigma_{aS}^i/\sigma_S^i$). We assume for simplicity that the incident power I_L is the same for all, even though generalizations for inhomogeneous (Gaussian) beams are also possible. The rate equation for the average phonon population n^i of a vibrational mode of *one molecule*, i, and its stationary state solution are given by expressions similar to eqn (3) and (5). The Stokes signal for this molecule is simply $I_S^i = \sigma_S^i I_L$, while the anti-Stokes signal is given by: $I_{aS}^i = n^i\sigma_{aS}^i I_L$. The anti-Stokes/Stokes ratio *for this molecule*, ρ^i, is given by an expression similar to eqn (7). If all the molecules experienced the same enhancements, then the total Stokes and anti-Stokes intensities would be $I_S = NI_S^i$ and $I_{aS} = NI_{aS}^i$, and the ratio would be $\rho = \rho^i$. However, if the molecules have different cross sections (SERS enhancements), which is a much more realistic assumption, we then have:

$$I_S = \sum_{i=1}^{N}\sigma_S^i I_L = N\langle\sigma_S\rangle I_L \tag{17}$$

and

$$\begin{aligned} I_{aS} &= \sum_{i=1}^{N}\sigma_{aS}^i I_L\left(\frac{\tau\sigma_S^i I_L}{\hbar\omega_L} + e^{-\hbar\omega_v/k_B T}\right) \\ &= N\langle\sigma_{aS}\sigma_S\rangle I_L\frac{\tau I_L}{\hbar\omega_L} + N\langle\sigma_{aS}\rangle I_L e^{-\hbar\omega_v/k_B T} \end{aligned} \tag{18}$$

All the averages here $\langle\cdots\rangle$ represent the usual statistical ensemble averages over the enhancement distribution. The aS/S-ratio is then:

$$\sigma = I_{aS}/I_S = \frac{\langle\sigma_{aS}\rangle}{\langle\sigma_S\rangle}\left[\frac{\langle\sigma_{aS}\sigma_S\rangle}{\langle\sigma_{aS}\rangle}\tau\frac{I_L}{\hbar\omega_L} + e^{-\hbar\omega_v/k_B T}\right] \tag{19}$$

Comparing this expression with that obtained previously in eqn (7), what we called the asymmetry factor A is now replaced by A^E (E for ensemble):

$$A^E = \frac{\langle\sigma_{aS}\rangle}{\langle\sigma_S\rangle} \tag{20}$$

Note that this is not exactly the average of the A^i's. Moreover, what we measure (instead of $\tau\sigma_S$) is now:

$$\tau\sigma_S^E = \tau\frac{\langle\sigma_{aS}\sigma_S\rangle}{\langle\sigma_{aS}\rangle} \tag{21}$$

To understand the meaning of σ_S^E, which we will call *the pumping cross-section*, we need to understand the sources of non-uniformity. The main source of variation is the large differences in SERS enhancements at different locations on the SERS substrate. We typically have values which are, say, 10^3–10^6 larger at hot-spots than in other places. However, for a given molecule, the ratio $A^i = \sigma_{aS}^i/\sigma_S^i$ is mostly determined by the change in the underlying plasmon resonance from

Stokes to anti-Stokes frequency. Since these resonances are typically broad, A^i should not vary that much (at least not by more than one order of magnitude). In fact, this ratio can (in a first approximation) be taken as a constant, which is an intrinsic property of the adsorbed molecule/metal complex.[10] Assuming that $A^i = A$ is the same for all molecules, we simply get that $A_E = A$, *i.e.* the A we measure is the correct one. Moreover, using $\sigma^i_{aS} = A\sigma^i_S$, we can express σ^E_S as a function of σ^i_S only, *i.e.*:

$$\sigma^E_S = \frac{\langle \sigma^2_S \rangle}{\langle \sigma_S \rangle} \tag{22}$$

If the distribution of σ_S's were fairly uniform (for example a Gaussian around an average value with a small standard deviation) then σ^E_S would be a good estimate of the average of the distribution (slightly overestimated). But this is far from reality in SERS conditions. A more realistic situation is to have a small number of molecules at hot-spots (HS), and a large number of molecules at non-HS (NHS) positions. If there is a difference of a few orders of magnitude between the cross sections σ^{HS}_S and σ^{NHS}_S, the numerator in eqn (25) is then easily dominated by the molecules at the HS (due to the square). For the denominator, it is not as clear-cut, it all depends on how much stronger the HS is and how many molecules there are at non-HS positions. This shows that $\sigma^E_S \sim \sigma^{HS}_S$, or perhaps slightly smaller. A more quantitative argument is only possible if we have a more realistic distribution of SERS enhancements for a given substrate, but the general qualitative conclusion is that *pumping experiments provide a good lower estimate (because of the influence of the rest of the distribution) of the cross section of the few molecules experiencing the highest enhancements.*

Photobleaching and pumping

The photostability of the probe *always* plays an important role in SERS and vibrational pumping is not an exception. Curiously enough, the "imperfection" introduced by photobleaching can be used as a tool to study the different averaging of the cross section in vibrational pumping conditions described in the previous Section. Ultimately, the outcome of an experiment is that an intensity is measured for either the Stokes or anti-Stokes signals of a peak at a given temperature T. The measured signal is already the averaged contribution of many molecules subject to a long-tail distribution. Doubtlessly, it is not easy to backtrack from the integrated values of the intensity to demonstrate that the Stokes and anti-Stokes signals are being averaged in different ways over the probability distribution of enhancements, because what is measured is already averaged and affected by additional parameters of the problem (like the asymmetry factor A, or the lifetime τ). We therefore need an additional tool to modify in some way this enhancement distribution. This is where the photostability of the probe can provide an additional insight into the vibrational pumping condition. It is a well known experimental fact that photobleaching in SERS occurs under conditions which depend primarily on the probe, the laser excitation wavelength, and the power density. Moreover, since photobleaching has generally an electromagnetic origin (it normally starts with absorption of a photon), it is also reasonable to assume that the photobleaching rate is linked to the electromagnetic (EM) enhancement. However, the real connection is not straightforward to analyze. One can think of many routes associated to the electromagnetic enhancement that might produce photobleaching. Direct absorption (in resonant or quasi-resonant) molecules is one option, but one could add to the list, in principle, two photon absorption, SERS vibrational pumping itself, *etc*. Vibrational pumping is unlikely to produce bleaching by itself, for it only achieves a small population (n) under typical SERS pumping conditions. But direct enhanced absorption (proportional to the enhancement experienced by the square of electric field of the laser $|E|^2$, rather than $|E|^4$ in the SERS enhancement) is the most likely cause.

Assuming that these facts are true, and regardless of the exact connection between the two phenomena, the photostability of the probe provides us with exactly the tool we need. It modifies the enhancement distribution as a function of time, simply by destroying the molecules with the highest enhancements, for which the bleaching rate is the fastest. It can, therefore, be used as a tool to probe the SERS enhancement factor distribution. A simple extrapolation of these facts to the vibrational pumping problem suggests that anti-Stokes signals under vibrational pumping conditions should bleach *at a different rate* from the Stokes counterparts. In fact, we can use this (somewhat circularly) to show that the bleaching rate is, effectively, linked to the enhancement. Fig. 6 shows the effect of photo-bleaching in the pumping and thermal-population dominated regimes. At room temperature, the system is in the thermally dominated regime and the anti-Stokes and Stokes signals are seen to decay while keeping their ratio approximately constant at $\sim$0.1. At 77 K, the system is in the *pumping dominated regime*. The anti-Stokes signal decays much faster than the Stokes one, and this results in a time-dependent ratio ρ. The Stokes signal decays slower at 77 K compared to 293 K, but this is related to the photobleaching effect itself and not to vibrational pumping. There are variations from point to point in the sample due to the inhomogeneity of the enhancement, but a rule of thumb is that the normalized (to $t = 0$) anti-Stokes signal decays much faster at 77 K than at 293 K, as shown in (c) due to the different physical origins of the anti-Stokes signals (vibrational pumping *vs*. normal thermal population), which imply a different averaging of the cross sections over the enhancement distribution, as shown in the previous section.

Fig. 7 shows a complementary result to demonstrate the effect of photobleaching under pumping conditions. The anti-Stokes signals at $T = 10$ K for (a) 647 nm, and (b) 514 nm laser excitations for the 610 cm^{-1} mode of RH6G are measured as a function of incident power density I_L. Both measurements are performed in the low-power density region, where the anti-Stokes signal is quadratic with incident power (as revealed, for example, in a log–log plot in the inset of Fig. 7(a), in which the data have a slope of 2 ± 0.1). The measurement is done with the shortest possible integration and total exposure times (1 s for each point). After the last point is taken, the sample is left for 15 min exposed to the laser. The power is turned off afterwards and the measurement is

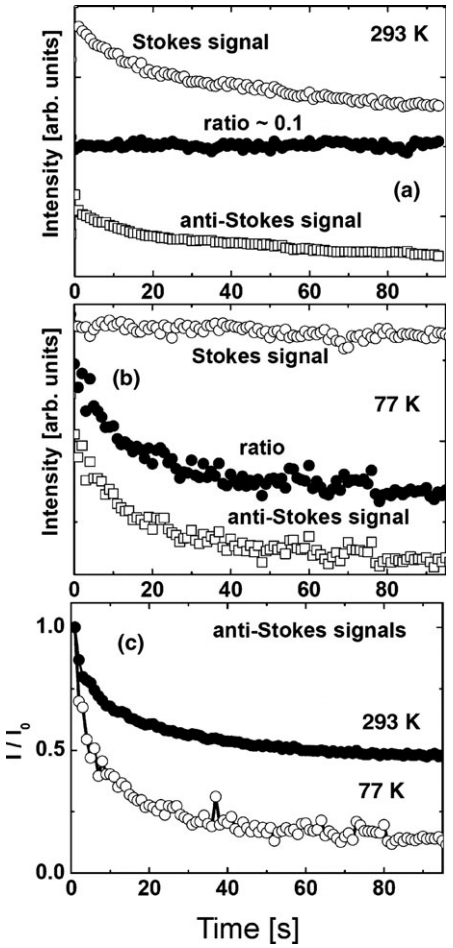

Fig. 6 Monitoring the Stokes and anti-Stokes intensities, and anti-Stokes/Stokes ratio under the action of photobleaching at (a) 293 K and (b) 77 K. (c) Direct comparison of the anti-Stokes intensity as a function of time at 293 and 77 K. Measurements are done for RH6G (610 cm^{-1} mode, 1 μM) on Ag (Lee and Meisel) colloids dried on Si and with 633 nm excitation. The ratio remains constant at 293 K while it varies at 77 K due to the faster bleaching of the anti-Stokes signal in the second case.

repeated. A "flatter" parabola with a much smaller coefficient implies an overall smaller pumping cross section, according to eqn (18). Even when photobleaching does not strongly affect the measurements itself (because the power level is low and the integration time is short) the accumulated effect of the exposure time in between the two measurements can be seen clearly. An estimation of cross sections from these data can give two completely different answers depending on the interplay between photobleaching, integration time, and exposure times. The overall message is then that *cross sections estimated by vibrational pumping have a meaning only within the constraints imposed by the photostability of the probe and the protocol used in the measurements*.

Total, radiative, and non-radiative cross sections

It is interesting to reflect at this stage on the meaning of the cross section in the present framework. Like in any scattering optical technique there is a *differential* radiative cross section for SERS ($d\sigma^R/d\Omega$); by integrating the differential cross-section over all

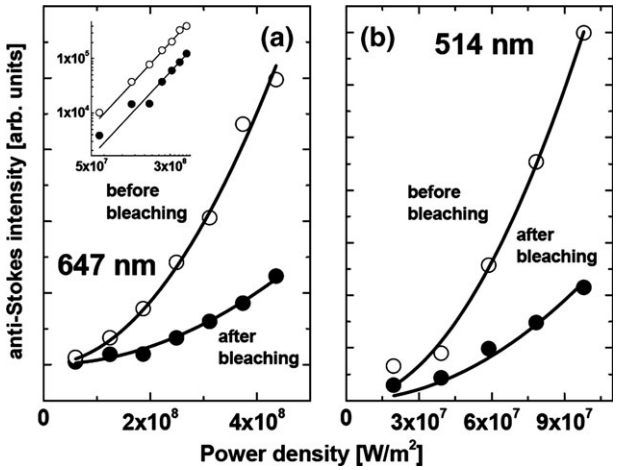

Fig. 7 Anti-Stokes signals (610 cm^{-1} mode of RH6G) at $T = 10$ K for two different laser excitations as a function of incident power density I_L: (a) 647 nm, and (b) 514 nm before and after the sample has been exposed to the effects of photo-bleaching for 15 minutes. At this temperature the anti-Stokes signal is completely dominated by pumping, and a (pure) quadratic power density dependence is expected.

detection directions it is possible to define the *integrated radiative SERS cross*-section $\int(d\sigma^R/d\Omega)d\Omega = \sigma^{SERS}$. The radiative cross section is directly linked to the intensity we see in the far-field as a Raman peak. As for the non-SERS case, this quantity is difficult to measure (it requires an integrating sphere, for example, to measure the intensity in all possible directions). But, in addition, σ^{SERS} is in general not as straightforward (as in the non-SERS case) to derive from the differential cross-section. There is an additional peculiarity to the SERS case which needs careful attention: because the metallic SERS substrate is optically absorbing, *some of the SERS scattered photons are absorbed and cannot be detected in the far-field*. This is a situation that would never arise in, for example, conventional Raman scattering of liquids. These events correspond to *non-radiative SERS processes*, where the SERS process *does* occur in the molecule (excitation of a vibration), but the Stokes-scattered photon is reabsorbed in the metal. The radiative SERS cross-section σ^{SERS} does not include such processes and is therefore not an exact representation of what is actually felt by the molecule (in terms of the number of vibrations created). We can therefore define a total SERS cross-section σ^T, which includes both radiative events and non-radiative ones (in all directions). One could argue that this distinction is irrelevant, since it is usually non-observable. However, this is the cross section that actually participates in SERS vibrational pumping! Hence one would expect, in general, that the cross section estimated by pumping *will overestimate the actual radiative cross section*. This issue becomes important when one tries to compare the pumping estimate with other estimates of the cross section derived by alternative routes. One such route is discussed in the following Section.

Advanced topics

A common problem in the quantification of enhancement factors and cross sections under SERS conditions is the lack

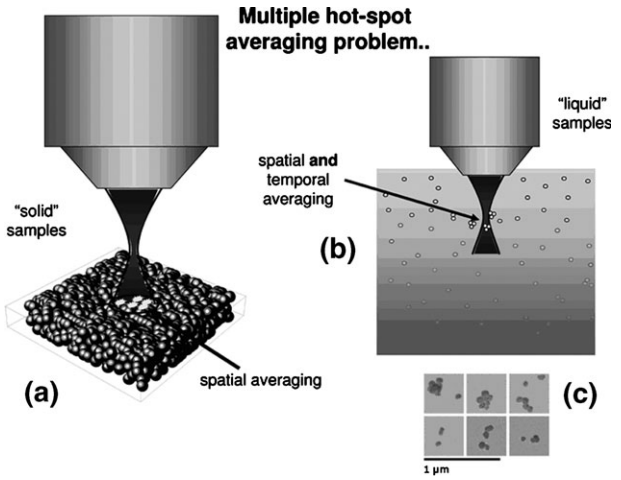

Fig. 8 SERS experiments in both "solid" and/or "liquid" samples (schematically represented in (a) and (b), respectively) produce signals which typically have contributions from a very inhomogeneous spatial averaging produced by hot-spots. The tail-like nature of the enhancement distribution[11] results in some extreme statistics where the contribution of a few single molecules at hot-spots (schematically shown in (a) as "white" dots) can have an overwhelming influence over the magnitude of the measured signal. In liquids—where clusters like those shown in (c) are diffusing all the time under the effect of Brownian motion and laser radiation forces[12]—the problem of temporal averaging over the integration time is added to the spatial averaging. It is typically *impossible* to know reliably how many molecules contributed to a given SERS signal in both cases. The signal could be dominated by a few molecules only, while the actual nominal concentration in the scattering volume of the collection optics may be 10^2–10^4 times larger. There could also be situations where the signal is contributed by a large number of molecules in relatively-low enhancement regions. The impossibility to distinguish one situation from the other makes (normally) the direct measurement of the SERS cross section an impossible task.

of knowledge of the number of molecules that produce the signal. The situation is depicted in Fig. 8 schematically, and accounts for the situations found in most "solid" SERS substrates as well as for "liquid" samples, where both spatial and temporal averaging are an issue. If we knew accurately the number of molecules producing the signal, there would be no need to utilize vibrational pumping as a means to estimate the SERS cross section.

As mentioned in the last two Sections, the "extreme statistics" of a few molecules contributing to a significant fraction of the signal is well understood from electromagnetic theory[13] and the *long-tail* nature of the probability distribution for the enhancement[13] around hot-spots. If we were able to pin down single molecule signals, we would then know the number of molecules ($N = 1$), and the estimation of the cross section is then direct; by comparison of the signal to a reference (calibrated) sample of known cross section. The question is now: how do we know we are in the single molecule limit? Very recently, a method based on the utilization of multiple analytes was developed to identify single molecule events unambiguously.[14,15] If we know now that the number of molecules producing the signal is *one*, and if *single molecule vibrational pumping* is observable for this one molecule, we will have an independent way of checking the pumping cross sections, and their interpretation. When we are dealing with only *one* molecule the problem of the spatial averaging of the cross section is also no longer an issue. The only remaining problems for the pumping cross section estimation are the uncertainty in the lifetime τ and the possible role of the non-radiative cross-section.

These topics—together with some miscellaneous recent developments in the field like pump-and-probe vibrational pumping—are, therefore, at the boundary of what has been done and understood in the field of SERS vibrational pumping as it stands at the time of writing this review. Hence, the content of the review from here onwards in this Advanced Topics section is speculative and largely unfinished. The justification for including here it is to show how the field is developing at the time of writing this review, and present a forward-looking perspective of possibilities ahead.

Single molecule vibrational pumping

In this section, we show the first attempts to combine the techniques of (i) the conclusive demonstration of SERS vibrational pumping at low temperatures described before,[16,17] and (ii) the introduction of a two-analyte technique (BiASERS)[14] to pin-down more reliably cases of single molecule (SM) SERS signals, to achieve what we call *single molecule (SM) SERS vibrational pumping*. The basic underlying idea is that the observation of SM-SERS pumping can provide, in principle, a unique possibility to double check estimates for the SERS cross sections using two completely different routes, in exactly *one and the same* measurement. As pointed out before in previous Sections, a key aspect of every vibrational pumping problem is the knowledge of the asymmetry factor (A). For single molecule events, the asymmetry parameter A cannot unfortunately be derived from a temperature dependent scan of the anti-Stokes/Stokes ratio (as done in all the examples shown before) due to issues of signal stability. With this proviso in mind, we demonstrate here that SM-SERS pumping could provide, in principle, the unique opportunity to estimate single molecule SERS cross sections in two different yet complementary ways.

Combining vibrational pumping with BiASERS

The bi-analyte SERS (BiASERS) method[14] provides an additional "degree of freedom" with respect to plain intensity fluctuation analysis[18] to pinpoint single molecule events in SERS. The method works as a "contrast technique" providing a background signal (from the partner dye) with which we can increase our statistical confidence in the identification of the true single molecule nature of SERS events. It has already been implemented in various conditions for that purpose.[19,20] Still, it is not without its limitations, which have been recently explored comprehensively together with the mathematical underpinnings for the analysis of single molecule fluctuations.[15] These techniques may be combined with low-temperature SERS pumping measurements to identify *single molecule vibrational pumping events*.

We proceed first with a description of the experimental phenomenology observed under the condition of SM-SERS

vibrational pumping, and provide the basic necessary elements for an interpretation of the data, as well as highlight the current problems.

Pumping of single molecules: typical experimental results

A schematic view of the experimental conditions used in SM-SERS pumping experiments can be seen in Fig. 9. We shall expedite here technical details of the experiment[21] to be able to reach the discussion of the main results observed to date. A beam and throughput characterization of the system with a reference is absolutely necessary for these experiments in order to calibrate the response of the system and deduce the cross section of a single molecule event from the measured Stokes intensity (in counts s^{-1}) with respect to a reference of known differential cross section. The beam characterization process with respect to a reference sample of known cross section has been described in full detail in ref. 11 (see the supplementary information in ref. 11).

Fig. 10 is a key result that shows that single molecule vibrational pumping can indeed be observed and combined with the power of BiASERS; the figure shows a series of selected spectra taken at 77 K, which allow the simultaneous observation of the $\sim$610 and $\sim$595 cm^{-1} modes of RH6G and Nile Blue (NB), respectively, on both the Stokes and anti-Stokes sides. The laser is scanned through the sample with 1 s integration time at each point and the spectra in Fig. 10 are selected cases from this scan which contains several thousand (typically $\sim$6000) spectra.[21] The vast majority of spectra contain no signal at all due to the sparsity of the clusters in these samples which are prepared with standard procedures.[14] The main result in Fig. 10 is the experimental fact that we can observe all possible combinations of different events combining the BiASERS concept[14] with vibrational pumping,[16]

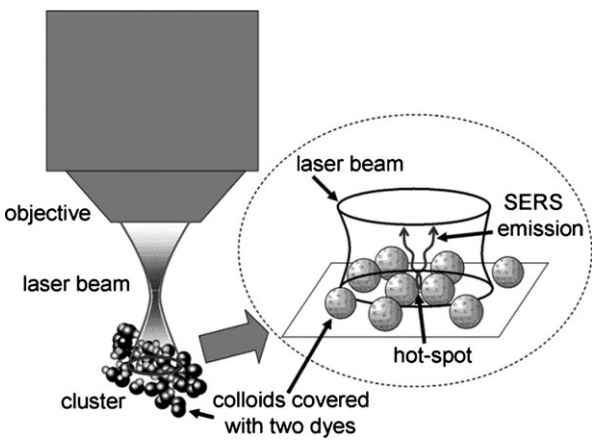

Fig. 9 Schematic representation of the SM-pumping BiASERS experiment. A $\times$50 long-working distance objective focuses a laser (633 nm at 2.8 mW with a spot area of 1.12 μm^2) on Ag-colloid clusters dried on a Si wafer (with polylysine[14]) and covered with RH6G and Nile Blue (NB) at 1 nM concentration (each). The sample is inside a cryostat for microscopy at 77 K. The blow-up on the right shows a detail of the sample with the colloids (covered with dyes), the beam, and a hot-spot emitting a SERS signal in the backscattered direction. These experiments show that it is possible to combine the concepts of two-analyte SERS (BiASERS) with vibrational pumping, to observe *single molecule vibrational pumping*.

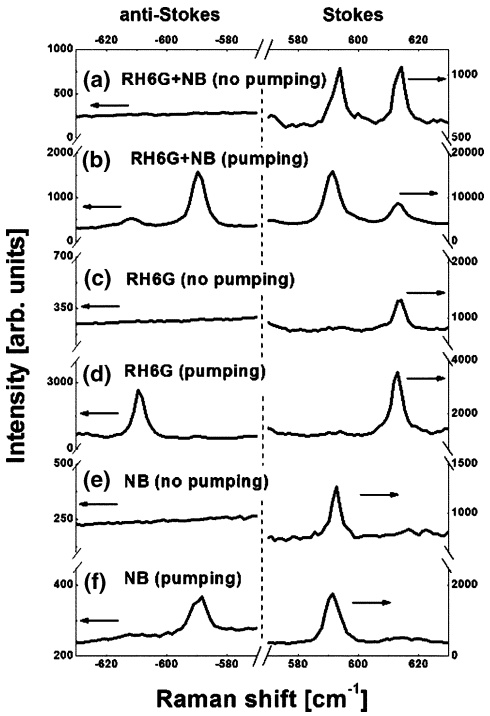

Fig. 10 BiASERS pumping events at 77 K at different places in the sample. The Stokes and anti-Stokes sides of the signals are measured simultaneously with a 1 s integration time. All possible combinations of cases can be seen under normal conditions: (a) RH6G + Nile Blue (NB) event with signal on the Stokes side but no pumping on the anti-Stokes, (b) RH6G + NB event with pumping for both dyes, (c) Stokes single molecule RH6G event without pumping, (d) single molecule RH6G event with pumping, (e) NB event without pumping, and (f) NB event with pumping.

i.e. (a) a case with RH6G + NB signals with no pumping on the anti-Stokes side, (b) RH6G + NB with pumping (several molecules at one or more hot-spots), (c) and (d) single molecule RH6G cases with and without pumping, and (e) and (f) NB single molecule cases with and without pumping, respectively. This clear experimental fact demonstrates that the technique of BiASERS can be combined with vibrational pumping.

The dispersion of the resonance

The effect of specific resonances affecting the Raman signals at the single molecule level and, ultimately, the result of SM-SERS pumping is very interesting in itself. Fig. 11 shows different events under the same experimental conditions of Fig. 10 but in a much wider energy range defined by a grating with lower dispersion (300 lines/mm), and at much lower incident power ($\sim$30 μW).

The main aim here is not to produce vibrational pumping but rather to reveal the different types of resonances these clusters have, and how they affect the Raman spectra (and the background) on energy scales comparable to the full Raman spectrum of these molecules. We can clearly see the presence and/or influence of different types of plasmon resonances in these clusters. Some resonances can be fairly localized in energy and are revealed on the Stokes side by their simultaneous effect on both the Raman peak intensities and the

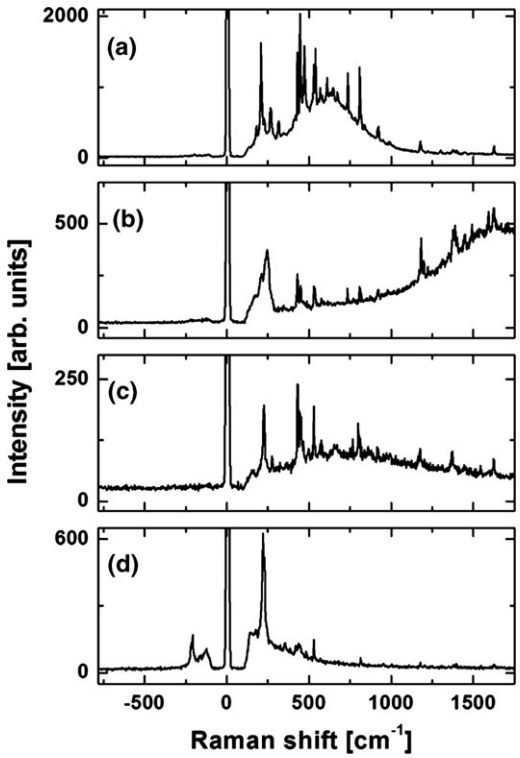

Fig. 11 Selected SERS spectra (of NB and CV) with evidence for the underlying resonance producing the enhancement. Note how different parts of the Raman spectrum are enhanced depending on where the resonance is actually centered. In (a) and (b), for example, either the low or high frequency Raman modes are enhanced. The spectra are taken at very low powers ($\sim$3 μW) to avoid photobleaching but still reveal the resonance on the Stokes side. At this power level, pumping on the anti-Stokes cannot be observed. See the text for further details.

background. The correlation between the effect of a resonance on the background *on the Stokes side* and the Raman signals on top of it has been noted several times in the past[22,23] and has been recently explained in terms of a *spectral modification of the surface enhanced fluorescence*[24] (which can be best studied in samples with much better controlled resonances, such as photolithographic arrays[24]).

The data in Fig. 11 demonstrates that peaks at highest Raman shifts ($\sim$1500 cm^{-1}) can have large asymmetries between the Stokes and anti-Stokes sides if the resonance is "localized" in energy and relatively narrow. For peaks closer to the laser, like the $\sim$595 and 610 cm^{-1} peaks of NB and RH6G, respectively, the problem will not be as serious but, still, it can justify a difference of a factor up to $\sim$10–20 between the Stokes and anti-Stokes cross sections.

A possible route is to try to characterize these resonances simultaneously with the SM-SERS pumping data. The simultaneous characterization of the resonance together with SERS spectra has been successfully attempted recently by Itoh *et al.*[25] In ref. 25, the simultaneous use of SERS with scattering measurements (using dark-field illumination) allows the characterization of the resonance affecting the Raman spectrum. The results from Itoh *et al.*[25] show a trend that could be successfully exploited for vibrational SM-SERS pumping in the future, in order to obtain the most accurate estimation of the asymmetry parameter A compatible with standard experimental conditions. There are many experimental challenges to resolve still, including the fact that experiments like those in ref. 25 are difficult to perform at low temperatures (needed for pumping) for they involve back illumination with a high numerical aperture (and short working distance) dark-field lens, which are typically incompatible with cryostats. Other options are being explored in our group at the time of writing this review.[21]

Single-molecule SERS pumping cross sections

Despite not having an accurate simultaneous determination of the asymmetry factors and the SM-SERS spectrum at this point in time, we are in a position to attempt a comparison between the estimations of single molecule SERS cross sections based on the Stokes signal and that obtained from vibrational pumping in the single molecule limit. Full details are given in ref. 11. Using reasonable estimates for the asymmetry parameter A (of no more than a factor of $\sim$10) it turns out that SM-SERS pumping cross section estimates are still larger than the SERS cross sections estimated by direct comparison with a reference compound[11] (and the fact that we have only one molecule). In a way, it is now easier to measure N than what it is to measure A, unlike the situation in the many-molecules limit described in all the previous sections.

This reaches then the boundary of what has been done and understood in SERS vibrational pumping at this stage and brings the review to an up-to-date point. The effects of spatial averaging of the enhancement are avoided in the single molecule limit and cannot be used as a justification for the difference. Several aspects are being explored at the moment of writing this review. We summarize them here very briefly for the sake of completeness (and in tentative order of importance): (i) Contributions to the pumping cross section by *non-radiative* processes, as described before. The possible effect of this contribution has been already noted in ref. 16 and is, in fact, one of the most likely sources of discrepancy between pumping and standard determinations of cross sections in single molecules. (ii) The possibility that the pumping cross section might include other pumping channels, besides the Stokes Raman processes. For example, *fluorescence pumping*, as described in ref. 26. There is in fact some experimental evidence at this stage (not shown) that suggests this is not an option, (iii) The possibility that the estimates of population lifetimes is still too inaccurate; a situation which will not be fully clarified until time-resolved SERS (and SM time-resolved SERS!) come of age. (iv) More speculative contributions to the pumping cross section, such as *coherent* anti-Stokes/Stokes scattering described by a few authors.[27,28] If coherent contributions were possible they cannot be described by a rate equation and would not be automatically included in eqn (3).

Our view at the moment of writing this review is that the cross section that pumps vibrations into the molecule *can have more than one origin simultaneously*. Fluorescence pumping[26] is a very serious candidate to add contributions, and one could envisage a transition from a "Raman dominated" to "fluorescence dominated" pumping situation (as described in ref. 26) depending on the resonance conditions which, in turn, are

affected by plasmon resonances. These possibilities, together with the possible role of non-radiative contributions to the cross section, mean that a great deal of additional work will have to be carried out before the true meaning of the SM-SERS cross section is fully understood.

Pump-and-probe vibrational pumping

Finally, one of the latest developments in the field of vibrational pumping has also been the demonstration of pump-and-probe experiments[21] which adds yet another additional available tool. The experiment is schematically shown in Fig. 12 (see caption to the figure). Basically, a weak "probe" laser under SERS vibrational pumping conditions (low temperatures) is present on the sample. An additional "pump" laser at a different wavelength (normally at longer wavelengths than the probe, to avoid any additional spurious emission from the pump) is overlapped on the same spot on the sample and its incident power controlled. The vibrational population produced by the "pump" is monitored as an increase in the anti-Stokes signals at the probe, as shown in Fig. 12. In this case, the signal at the anti-Stokes of the probe is expected to rise *linearly* with the pump intensity, as it is indeed observed in Fig. 12. All experiments have to be performed at low temperatures ($T = 10$ K in our case) in the regime where the population of vibrations is no longer determined by thermal effects but rather by the pumping rate produced the lasers.

An anti-Stokes photon at the probing laser will only be observed if a molecule is already excited by the pump *or* the probe. The probe will inevitably produce a small amount of *self-pumping* in the vibration. If we subtract the anti-Stokes peak with only the probe laser active, from the one with both lasers, we will therefore have the spectra of photons resulting from *an anti-Stokes process at the probe resulting from vibrations that have been created by the pump*.

The population n created by the simultaneous effect of pump + probe is:

$$n = \frac{\tau\sigma_{\mathrm{S}}^{\mathrm{pump}} I^{\mathrm{pump}}}{\hbar\omega^{\mathrm{pump}}} + \frac{\tau\sigma_{\mathrm{S}}^{\mathrm{probe}} I^{\mathrm{probe}}}{\hbar\omega^{\mathrm{probe}}} \tag{23}$$

where $\sigma_{\mathrm{S}}^{\mathrm{pump,probe}}$ and $I^{\mathrm{pump,probe}}$ are the Stokes cross sections and power densities [W m^{-2}] at the pump and probe wavelengths, respectively, and τ is the population lifetime of the mode defined before.

If N is the number of molecules at the overlapping region between the two spots, the intensity of the anti-Stokes peak of the probing laser (with both lasers on) is therefore:

$$I_{\mathrm{aS}} = N\tau\left[\frac{\langle\sigma_{\mathrm{S}}^{\mathrm{pump}}\sigma_{\mathrm{aS}}^{\mathrm{probe}}\rangle I^{\mathrm{pump}}}{\hbar\omega^{\mathrm{pump}}} + \frac{\langle\sigma_{\mathrm{S}}^{\mathrm{probe}}\sigma_{\mathrm{aS}}^{\mathrm{probe}}\rangle I^{\mathrm{probe}}}{\hbar\omega^{\mathrm{probe}}}\right] I^{\mathrm{probe}} \tag{24}$$

where the brackets $\langle\cdots\rangle$ mean, as before, spatial averaging over the distribution of enhancements at the different molecules in the illuminated area. This last expression produces the expected quadratic intensity dependence of the anti-Stokes for the *self-pumping events* of the probe (second term), but it also produces a *linear* intensity dependence on the pump intensity, produced by the "cross-talking" between the effects of the two lasers (first term). The first term in eqn (24) monitors then (through anti-Stokes processes at the probe) vibrations that

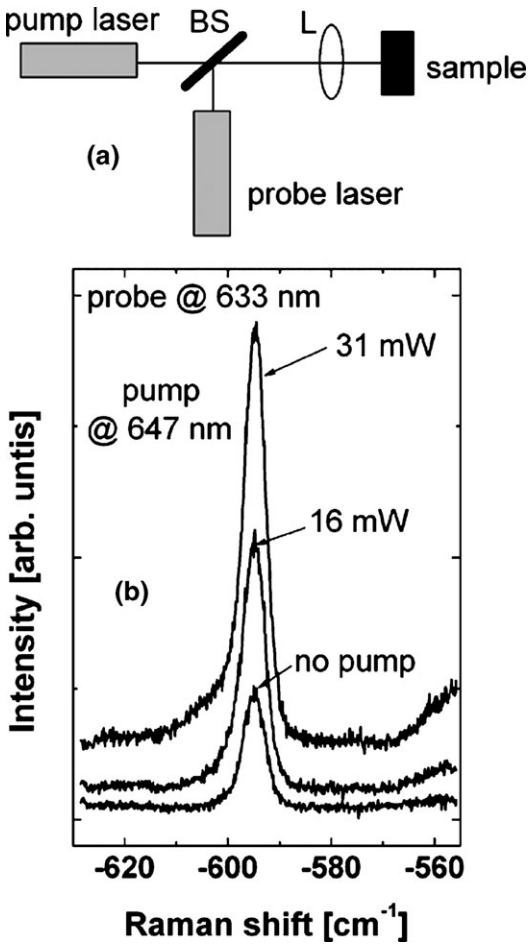

Fig. 12 (a) A schematic representation of the SERS vibrational pump-and-probe experiment. A weak probe laser (~3 mW) is overlapped with a pump laser (~0–60 mW) over the same spot (~15 μm in diameter) with the help of a beam-splitter (BS) and a lens (L). The sample is inside a cryostat for optical experiments at $T = 10$ K. In this case, the anti-Stokes signal of the 595 cm^{-1} mode of Nile Blue (NB) is collected with a high numerical aperture zoom lens and measured with a high-resolution double additive spectrometer coupled to a liquid nitrogen cooled CCD detector. The spectra in (b) show a specific example of vibrational pump-and-probe. When the pump is off (at 647 nm), the anti-Stokes signal at 633 nm shows a peak which is the self-pumping of the probe at 633 nm. If the pump laser is now increased, the vibrations being pumped at 647 nm are monitored on the anti-Stokes side at 633 nm, with a peak increasing linearly with the pump power. The slope of this linear increase is directly linked to how much overlap there is (in terms of the underlying plasmon resonances and spatial distribution in the system) between the wavelengths of the pump and the probe. See the text for further details.

are created by the pump. The intensity of the anti-Stokes peak *with only the probing laser on is*:

$$I_{\mathrm{aS}}^{0} = N\tau\frac{\langle\sigma_{\mathrm{S}}^{\mathrm{probe}}\sigma_{\mathrm{aS}}^{\mathrm{probe}}\rangle I^{\mathrm{probe}}}{\hbar\omega^{\mathrm{probe}}} I^{\mathrm{probe}} \tag{25}$$

Hence, by taking the difference of these two intensities, we obtain:

$$\Delta I_{\mathrm{aS}} = N\tau\frac{\langle\sigma_{\mathrm{S}}^{\mathrm{pump}}\sigma_{\mathrm{aS}}^{\mathrm{probe}}\rangle I^{\mathrm{pump}}}{\hbar\omega^{\mathrm{pump}}} I^{\mathrm{probe}} \tag{26}$$

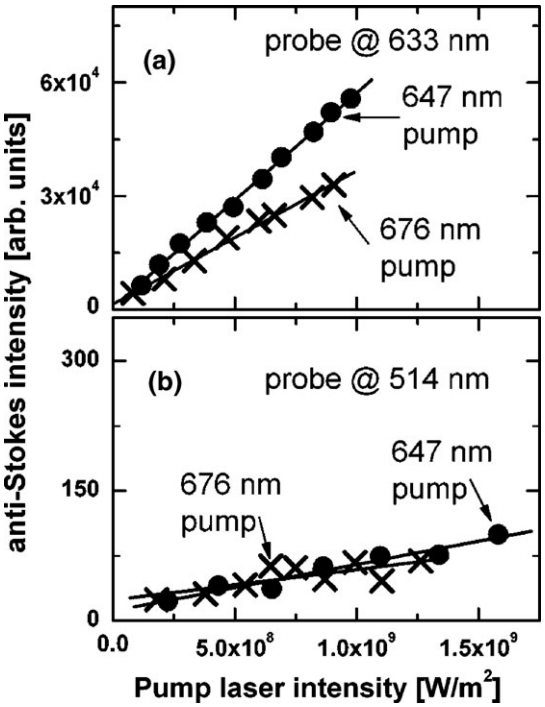

Fig. 13 Excess anti-Stokes signal (subtracting the self-pumping of the probe) for the 595 cm^{-1} anti-Stokes peak of NB as a function of pump laser power density. In (a) the probing laser is the 633 nm line whilst data is shown for both the 647 and 676 nm pumping lines, respectively. In (b) we show the same situation but for 514 nm probe, *i.e.* a much wider ''detuning'' between the pump and probe wavelengths. The slope of the power dependencies in (b) are about $\sim$500 times smaller than in (a) accounting for the detuning in the simultaneous resonance conditions of both lasers with respect to the available resonances in this system and their spatial distribution. See the text for further details.

which is the *excess* anti-Stokes signal ΔI_{aS}, measured in Fig. 13 for different pump and probe combinations.

The pump-and-probe vibrational SERS pumping technique is completely new and, therefore, we shall not dwell into too many details here. It is interesting to note that it is one of the few cases we are aware of in which ''cross-talking'' between the effects of two lasers can be achieved through the incoherent Raman population of a vibrational level. The meaning of the effect of the ''pump'' on the ''probe'' signal in this technique will strongly depend on the pumping mechanism responsible and the experimental conditions. If the probe can produce either fluorescence or Raman pumping, the meaning of the effect on the probe will be different in one case or the other. In addition, if all the molecules are exactly equivalent and subject to the same type of plasmon resonance, the effect of different pump lasers could be used, in principle, to measure the *dispersion* (wavelength dependence) of the resonance producing the pumping. If, on the contrary, different wavelengths of the pump laser are linked to resonances that have different *spatial distributions* on the sample, the different slopes of the probe signals for different pumps (seen in Fig. 13) also have information on the spatial averaging and overlap of the resonances (eqn (26)). This is undoubtedly an interesting new development in the field, albeit with many experimental challenges of its own.

Conclusions

The field of SERS vibrational pumping has progressed enormously in the last ten years. Arguably, this review condenses everything that has been done to date in the field of SERS vibrational pumping. As it stands today, the field faces new challenges which are comparable (or more difficult) than the original questions. There has yet to be a thorough understanding of the different regimes of vibrational pumping (Raman pumping, fluorescence pumping, resonance effects, *etc*...). In addition the development of experimental tools and experimental conditions that will facilitate reproducibility continues to be hugely important. Control of plasmon resonances, experimental estimations of lifetimes, single molecule SERS pumping, pump-and-probe pumping, *etc*... are all major challenges ahead. If the unpredictable (and sometimes painfully slow) development of SERS as a technique in the last couple of decades serves as an example to the future, it might take possibly another decade before all the principles of SERS vibrational pumping (and in particular vibrational pumping at the single molecule level) are pinned down and understood in their full details. It is the hope of the present authors that this review of the basic principles (and the state-of-the-art and current trends) will stimulate more debate and further work in this fascinating (and fundamental) aspect of vibrational spectroscopy of molecules.

Acknowledgements

R. C. M. acknowledges partial support from the National Physical Laboratory (NPL, UK) and the hospitality of the MacDiarmid Institute at Victoria University of Wellington (VUW), New Zealand. P. G. E. and E. C. L. R. acknowledge support for this work from the Royal Society of New Zealand (RSNZ) under a Marsden Grant. P. G. E. and L. F. C. acknowledge support from the EPSRC GR/T0612. We are indebted to Matthias Meyer (VUW-NZ) for help during the experiments and useful discussions.

References

1 K. Kneipp, Y. Wang, H. Kneipp, I. Itzkan, R. R. Dasari and M. S. Feld, *Phys. Rev. Lett*., 1996, **76**, 2444–2447.
2 K. Kneipp and H. Kneipp, *Faraday Discuss*., 2006, **132**, 27–33.
3 T. L. Haslett, L. Tay and M. Moskovits, *J. Chem. Phys*., 2000, **113**, 1641–1646.
4 A. G. Brolo, A. C. Sanderson and A. P. Smith, *Phys. Rev. B*, 2004, **69**, 045424.
5 E. C. Le Ru and P. G. Etchegoin, *Faraday Discuss*., 2006, **132**, 63–75.
6 M. Moskovits, L. Tay, J. Yang and T. L. Haslett, *Top. Appl. Phys*., 2002, **82**, 215.
7 A. Laubereau and W. Kaiser, *Rev. Mod. Phys*., 1978, **50**, 607–665.
8 Demtroder, *Laser Spectroscopy*, Springer Verlag, Berlin, 2003.
9 P. C. Lee and D. Meisel, *J. Phys. Chem*., 1982, **86**, 3391.
10 R. C. Maher, J. Hou, L. F. Cohen, E. C. Le Ru, J. M. Hadfield, J. E. Harvey, P. G. Etchegoin, F. M. Liu, M. Green, R. J. C. Brown and M. J. T. Milton, *J. Chem. Phys*., 2005, **123**, 084702.

11 E. C. Le Ru, E. Blackie, M. Meyer and P. G. Etchegoin, *J. Phys. Chem. C*, 2007, **111**, 13794.
12 H. X. Xu and M. Kall, *Phys. Rev. Lett.*, 2002, **89**, 246802.
13 E. C. Le Ru, P. G. Etchegoin and M. Meyer, *J. Chem. Phys.*, 2006, **125**, 204701.
14 E. C. Le Ru, M. Meyer and P. G. Etchegoin, *J. Phys. Chem. B*, 2006, **110**, 1944–1948.
15 P. G. Etchegoin, M. Meyer, E. Blackie and E. C. Le Ru, *Anal. Chem.*, 2007, **79**, 8411.
16 R. C. Maher, L. F. Cohen, E. C. Le Ru and P. G. Etchegoin, *J. Phys. Chem. B*, 2006, **110**, 19469–19478.
17 R. C. Maher, P. G. Etchegoin, E. C. Le Ru and L. F. Cohen, *J. Phys. Chem. B*, 2006, **110**, 11757–11760.
18 P. G. Etchegoin, M. Meyer and E. C. Le Ru, *Phys. Chem. Chem. Phys.*, 2007, **9**, 3006–3010.
19 Y. Sawai, B. Takimoto, H. Nabika, K. Ajito and K. Murakoshi, *J. Am. Chem. Soc.*, 2007, **129**, 1658–1662.
20 P. J. G. Goulet and R. F. Aroca, *Anal. Chem.*, 2007, **79**, 2728–2734.
21 P. G. Etchegoin, M. Meyer, C. Galloway and E. C. Le Ru, unpublished work.
22 E. C. Le Ru, M. Dalley and P. G. Etchegoin, *Curr. Appl. Phys.*, 2006, **6**, 411–414.
23 E. C. Le Ru, P. G. Etchegoin, J. Grand, N. Felidj, J. Aubard, G. Levi, A. Hohenau and J. R. Krenn, *Curr. Appl. Phys.*, 2008, **8**, 467.
24 E. C. Le Ru, P. G. Etchegoin, J. Grand, N. Felidj, J. Aubard and G. Levi, *J. Phys. Chem. C*, 2007, **111**, 16076.
25 T. Itoh, K. Yoshida, V. Biju, Y. Kikkawa, M. Ishikawa and Y. Ozaki, *Phys. Rev. B*, 2007, **76**, 085405.
26 H. X. Xu, X. H. Wang, M. P. Persson, H. Q. Xu, M. Kall and P. Johansson, *Phys. Rev. Lett.*, 2004, **93**, 243002.
27 I. Baltog, M. Baibarac and S. Lefrant, *Physica E*, DOI: 10.1016/j.physe.2007.07.022.
28 S. K. Potapov, V. L. Derbov and A. F. Bukatin, *J. Appl. Spectrosc.*, 1985, **42**, 76.